DOI: 10.1021/ic900609e

Inorganic Chemistry
Article

Structural Variations within Group 1 $(Li-Cs)^+$(2,2,6,6-Tetramethyl-1-piperidinyloxy)$^-$ Complexes Made via Metallic Reduction of the Nitroxyl Radical

Liam Balloch, Allison M. Drummond, Pablo García-Álvarez, David V. Graham, Alan R. Kennedy, Jan Klett, Robert E. Mulvey,* Charles T. O'Hara,* Philip J. A. Rodger, and Iain D. Rushworth

WestCHEM, Department of Pure and Applied Chemistry, University of Strathclyde, Glasgow G1 1XL, U.K.

Received March 30, 2009

Treatment of 2,2,6,6-tetramethyl-1-piperidinyloxy (TEMPO) with a group 1 metal (Li, Na, K, Rb, or Cs), resulted in the reduction of this important radical to the $TEMPO^-$ anion—the first examples of elemental-metal single electron reduction of the radical to its anionic form. The synthesis and characterization of seven alkali metal $TEMPO^-$ complexes are reported. A variety of structural motifs are encountered depending on the choice of metal and/or solvent. $(THF)_2 \cdot [Li^+(TEMPO^-)]_4$ **1** crystallized from THF as a cyclic (Li_4O_4) molecule. Two Li centers are stabilized by coordination to a THF molecule; the others by intramolecular coordination to N_{TEMPO} atoms. $[(THF) \cdot Na^+(TEMPO^-)]_4$ **2** exists as a distorted cubane where each Na center is coordinated to a THF molecule. No appreciable $Na-N_{TEMPO}$ coordination is observed. $[(THF)_2 \cdot Na_3^+(TEMPO^-)_2(OH)]_2$ **3** was serendipitously prepared and exists as a distorted bis(cubane). It is envisaged that **3** is formed from **2** by insertion of a $(Na\text{-}OH)_2$ double bridge into its framework. $[Na_4^+(\mu_3\text{-}TEMPO^-)_2(\mu_2\text{-}TEMPO^-)_2(TMEDA)_2]$ **4**, adopts a four-runged ladder structure, whereby the two outer Na centers are coordinated to TMEDA, in addition to two μ_2-O and a N atom. The inner metal atoms are bound to three μ_3-O atoms and a N atom. $[(THF) \cdot K^+(TEMPO^-)]_4$ **5** resembles the motif found for **2**; however, presumably because of the larger size of the metal, $K-N_{TEMPO}$ interactions are present in **5**. The asymmetric unit of $[(TMEDA) \cdot Rb_2^+(TEMPO^-)_2]_2$ **6** comprises a Rb_4O_4 cubane with half a molecule of TMEDA coordinated to each metal. From a supramolecular perspective, **6** exists as a polymeric array of cubane units connected by TMEDA bridges. Completing the series, $[Cs^+(TEMPO)]_\infty$ **7** crystallizes from hexane to form a donor-free polymeric complex. Complexes **1**, **2**, and **4**–**7** are soluble in D_8-THF solution, and their NMR spectra are reported. The solution structures in donor solvent appear virtually identical.

Introduction

TEMPO (2,2,6,6-tetramethyl-1-piperidinyloxy) is a stable nitroxyl free radical which continues to draw an extraordinary degree of interest.[1,2] First synthesized by Lebelev and Kazarnowskii in 1960,[3] the radical has found many applications in organic and polymer synthesis, including the oxidation of amines, phosphines, anilines, phenol, but perhaps most importantly primary and secondary alcohols.[4−13] TEMPO is also used as a probe for biological systems using electron spin resonance spectroscopy and for trapping other radicals. Studer et al. have elegantly shown that oxidative homocoupling of Grignard reagents in the presence of TEMPO and dioxygen is possible in high yields.[14] Perhaps most pertinent to this study, the radical has also been utilized in coordination chemistry, yielding an interesting and varied selection of ligation modes, as well as flexibility in the ligand's electronic structure. The bulk of TEMPO coordination chemistry lies with the d-block metals (such as Ti,[15−17] Mn,[18,19]

*To whom correspondence should be addressed. E-mail: charlie.ohara@strath.ac.uk.

(1) Barriga, S. *Synlett* **2001**, *4*, 563.
(2) De Souza, M. V. N. *Mini-Rev. Org. Chem.* **2006**, *3*, 155–165.
(3) Lebelev, O. L.; Kazarnovskii, S. N. *Zhur. Obshch. Khim.* **1960**, *30*, 1631.
(4) Bragd, P. L.; van Bekkum, H.; Besemer, A. C. *Top. Catal.* **2004**, *27*, 49–66.
(5) Guo, Y. C.; Zhao, J. F.; Xu, J. X.; Wang, W.; Tian, F. S.; Yang, G. Y.; Song, M. P. *J. Nat. Gas Chem.* **2007**, *16*, 210–212.
(6) Herath, A. C.; Becker, J. Y. *Electrochim. Acta* **2008**, *53*, 4324–4330.
(7) Kumar, R. S.; Karthikeyan, K.; Perumal, P. T. *Can. J. Chem.* **2008**, *86*, 720–725.
(8) Liu, Z. Q.; Shang, X. J.; Chai, L. Z.; Sheng, Q. J. *Catal. Lett.* **2008**, *123*, 317–320.
(9) Minisci, F.; Recupero, F.; Pedulli, G. F.; Lucarini, M. *J. Mol. Catal. A: Chem.* **2003**, *204*, 63–90.
(10) Sheldon, R. A.; Arends, I. *Adv. Synth. Catal.* **2004**, *346*, 1051–1071.
(11) Sheldon, R. A.; Arends, I.; Ten Brink, G. J.; Dijksman, A. *Acc. Chem. Res.* **2002**, *35*, 774–781.
(12) Wang, X. L.; Liu, R. H.; Jin, Y.; Liang, X. M. *Chem.—Eur. J.* **2008**, *14*, 2679–2685.
(13) Zhan, B. Z.; Thompson, A. *Tetrahedron* **2004**, *60*, 2917–2935.
(14) Maji, M. S.; Pfeifer, T.; Studer, A. *Angew. Chem., Int. Ed.* **2008**, *47*, 9547.
(15) Mahanthappa, M. K.; Cole, A. P.; Waymouth, R. M. *Organometallics* **2004**, *23*, 836–845.
(16) Mahanthappa, M. K.; Huang, K. W.; Cole, A. P.; Waymouth, R. M. *Chem. Commun.* **2002**, 502–503.
(17) Schröder, K.; Haase, D.; Saak, W.; Beckhaus, R.; Kretschmer, W. P.; Lutzen, A. *Organometallics* **2008**, *27*, 1859–1868.
(18) Dickman, M. H.; Porter, L. C.; Doedens, R. J. *Inorg. Chem.* **1986**, *25*, 2595–2599.
(19) Jaitner, P.; Huber, W.; Huttner, G.; Scheidsteger, O. *J. Organomet. Chem.* **1983**, *259*, C1–C5.

Published on Web 05/21/2009

Scheme 1. Radical (left) and Anionic (right) Forms of the TEMPO Ligand

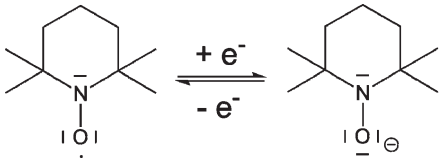

Co,[20,21] Ni,[22] Cu,[23−26] Zn,[27] Mo,[28] Ru,[29−31] Rh,[32,33] Pd[34,35] and Hg[36]). Recently, TEMPO complexes of the s-, p-, and f-block have been structurally characterized. In 2001, we revealed that TEMPO could behave as a "chameleonic ligand" toward s-block metal amides, that is, it can retain its radical nature or be reduced to an anionic entity in different ligation modes depending on the composition of the s-block metal amide (Scheme 1).[37] As well as coordinating to a metal center as an anion or as a radical, the TEMPO unit can act solely as an O donor (η^1) or as a bidentate N/O donor (η^2).

Moving to the p-block metals, TEMPO complexes of Al,[38] Ga,[38] Ge,[39−41] and Sn[39] have been isolated. Evans et al., prepared the first TEMPO complex of a lanthanide element [also the first per(TEMPO) complex], $Sm_2(TEMPO)_6$.[42] This complex is particularly relevant to this study as the complex can be considered as per(TEMPO) species with respect to the anionic ligands. Here we report the synthesis and characterization of a complete series of alkali metal (Li, Na, K, Rb, and Cs) TEMPO complexes, prepared directly from the parent alkali metal. To the best of our knowledge these reactions represent the first elemental-metal reduction of the nitroxyl radical TEMPO to its anionic form although the $TEMPO^-$ anion has been generated in other ways.[15−36]

Experimental Section

General Information. All reactions and manipulations were carried out in an atmosphere of dry, pure argon gas, using standard Schlenk protocols. Hexane and tetrahydrofuran (THF) were freshly distilled over Na/benzophenone. NMR samples were prepared under a protective atmosphere inside a glovebox using D_8-THF solvent (which was degassed using freeze−pump−thaw cycles, and pre-dried over a 4 Å molecular sieve). Elemental Li, Na, K, Rb, and Cs were procured from either Sigma-Aldrich or Strem Chemicals and were used as received. All NMR spectra were measured on a Bruker DPX400 or AMX400 spectrometer. The X-ray structural determinations were carried out on a Nonius Kappa diffractometer with a CCD area detector using graphite-monochromated $Mo_{K\alpha}$ radiation. Because of the extreme air- and moisture sensitivity of **1**, **2** and **4**−**7** reproducible elemental analyses could not be obtained.

Synthesis of $(THF)_2\cdot[Li^+(TEMPO^-)]_4$ (1). Lithium powder (0.21 g, 30 mmol) was suspended in freshly distilled THF (30 mL) in a flame-dried Schlenk tube. TEMPO (4.68 g, 30 mmol) was introduced via a solid addition tube. The TEMPO dissolved immediately producing a vivid orange color. This mixture was heated to reflux for 100 h, during which time a gradual discoloration of the solution and precipitation of an off-white solid was observed. This precipitate was isolated by Schlenk filtration, and the mother liquor was cooled to −30 °C for 48 h to yield a crop of X-ray quality colorless needle-like crystals of **1** (NMR spectroscopic analysis confirmed that the off-white precipitate and crystalline material were the same product). The combined yield of crystals and precipitate was 35% (2.09 g). ^{1}H NMR (D_8-THF, 400 MHz, 300 K): δ 1.46 (β-H and γ-H, 6H, br s), 1.11 (CH_3, 12H, br s). ^{13}C NMR (D_8-THF, 100 MHz, 300 K): 58.9 (α-*C*), 41.2 (*β*-*C*), 34.3 (CH_3), 19.2 (*γ*-*C*), 18.6 (CH_3) *N.B.* THF lost on isolation.

Synthesis of $[(THF)\cdot Na^+(TEMPO^-)]_4$ (2). A Schlenk tube was charged with freshly cleaned elemental sodium (0.23 g, 10 mmol). To enhance the reactivity of the metal, the sodium was melted to a mirror using a heat gun. THF (30 mL) and TEMPO (1.56 g, 10 mmol) were then added, and this orange-colored mixture was heated to reflux for 48 h. The solution was cooled to −20 °C for 48 h to precipitate a large crop of colorless crystals of **2** (1.18 g, 47%). ^{1}H NMR (D_8-THF, 400 MHz, 300 K): δ 1.45 (β-H and γ-H, 6H, br s), 1.10 (CH_3, 12H, br s). ^{13}C NMR (D_8-THF, 100 MHz, 300 K): 58.5 (α-*C*), 41.4 (*β*-*C*), 34.6 (CH_3), 18.8 (*γ*-*C*), 18.8 (CH_3).

Synthesis of $[(THF)_2\cdot Na_3^+(TEMPO^-)_2(OH)]_2$ (3). A Schlenk tube was charged with sodium spheres (0.23 g, 10 mmol). THF (30 mL) and TEMPO (1.56 g, 10 mmol) were then added, and this orange-colored mixture was heated to reflux for 48 h. The solution was cooled to −20 °C for 72 h to precipitate a small crop of colorless crystals of **3** (yield $< 5\%$). It is thought that the hydroxide contaminant was due to the tarnished surface of the metallic spheres (presumably contaminated with oxygen-based species) resulting in the formation of a sodium mirror which was of poor quality.

Synthesis of $Na^+(TEMPO)^-$ Powder. A Schlenk tube was charged with freshly cleaned elemental sodium (0.46 g, 20 mmol). To enhance the reactivity of the metal, the sodium was melted to a mirror using a heat gun. Hexane (40 mL) and TEMPO (3.12 g, 20 mmol) were added to the Schlenk tube, and this orange-colored mixture was heated to reflux for 12 h, resulting in the precipitation of a white solid. On reducing the solvent in vacuo by approximately 50%, further precipitation occurred. The solid was collected by filtration. Typical yield: 2.3 g, 65%.

(20) Dickman, M. H. *Acta Crystallogr., Sect. C: Cryst. Struct. Commun.* **1997**, *53*, 1192–1195.
(21) Jaitner, P.; Huber, W.; Gieren, A.; Betz, H. *J. Organomet. Chem.* **1986**, *311*, 379–385.
(22) Mindiola, D. J.; Waterman, R.; Jenkins, D. M.; Hillhouse, G. L. *Inorg. Chim. Acta* **2003**, *345*, 299–308.
(23) Caneschi, A.; Grand, A.; Laugier, J.; Rey, P.; Subra, R. *J. Am. Chem. Soc.* **1988**, *110*, 2307–2309.
(24) Dickman, M. H.; Doedens, R. J. *Inorg. Chem.* **1981**, *20*, 2677–2681.
(25) Laugier, J.; Latour, J. M.; Caneschi, A.; Rey, P. *Inorg. Chem.* **1991**, *30*, 4474–4477.
(26) Porter, L. C.; Dickman, M. H.; Doedens, R. J. *Inorg. Chem.* **1983**, *22*, 1962–1964.
(27) Grirrane, A.; Resa, I.; Rodriguez, A.; Carmona, E.; Alvarez, E.; Gutierrez-Puebla, E.; Monge, A.; Galindo, A.; del Rio, D.; Andersen, R. A. *J. Am. Chem. Soc.* **2007**, *129*, 693–703.
(28) Jaitner, P.; Huber, W.; Gieren, A.; Betz, H. *Z. Anorg. Allg. Chem.* **1986**, *538*, 53–60.
(29) Cogne, A.; Belorizky, E.; Laugier, J.; Rey, P. *Inorg. Chem.* **1994**, *33*, 3364–3369.
(30) Handa, M.; Sayama, Y.; Mikuriya, M.; Nukada, R.; Hiromitsu, I.; Kasuga, K. *Bull. Chem. Soc. Jpn.* **1995**, *68*, 1647–1653.
(31) Seyler, J. W.; Fanwick, P. E.; Leidner, C. R. *Inorg. Chem.* **1992**, *31*, 3699–3700.
(32) Dong, T. Y.; Hendrickson, D. N.; Felthouse, T. R.; Shieh, H. S. *J. Am. Chem. Soc.* **1984**, *106*, 5373–5375.
(33) Felthouse, T. R.; Dong, T. Y.; Hendrickson, D. N.; Shieh, H. S.; Thompson, M. R. *J. Am. Chem. Soc.* **1986**, *108*, 8201–8214.
(34) Dickman, M. H.; Doedens, R. J. *Inorg. Chem.* **1982**, *21*, 682–684.
(35) Porter, L. C.; Doedens, R. J. *Acta Crystallogr., Sect. C: Cryst. Struct. Commun.* **1985**, *41*, 838–840.
(36) Haneline, M. R.; Gabbaï, F. P. *Inorg. Chem.* **2005**, *44*, 6248–6255.
(37) Forbes, G. C.; Kennedy, A. R.; Mulvey, R. E.; Rodger, P. J. A. *Chem. Commun.* **2001**, 1400.
(38) Jones, C.; Rose, R. P. *New J. Chem.* **2007**, *31*, 1484–1487.
(39) Iwamoto, T.; Masuda, H.; Ishida, S.; Kabuto, C.; Kira, M. *J. Am. Chem. Soc.* **2003**, *125*, 9300.
(40) Naka, A.; Hill, N. J.; West, R. *Organometallics* **2004**, *23*, 6330–6332.
(41) Spikes, G. H.; Peng, Y.; Fettinger, J. C.; Steiner, J.; Power, P. P. *Chem. Commun.* **2005**, 6041–6043.
(42) Evans, W. J.; Perotti, J. M.; Doedens, R. J.; Ziller, J. W. *Chem. Commun.* **2001**, 2326–2327.

Scheme 2. Preparation of the Alkali Metal TEMPO Complexes (**1**−**7**)[a]

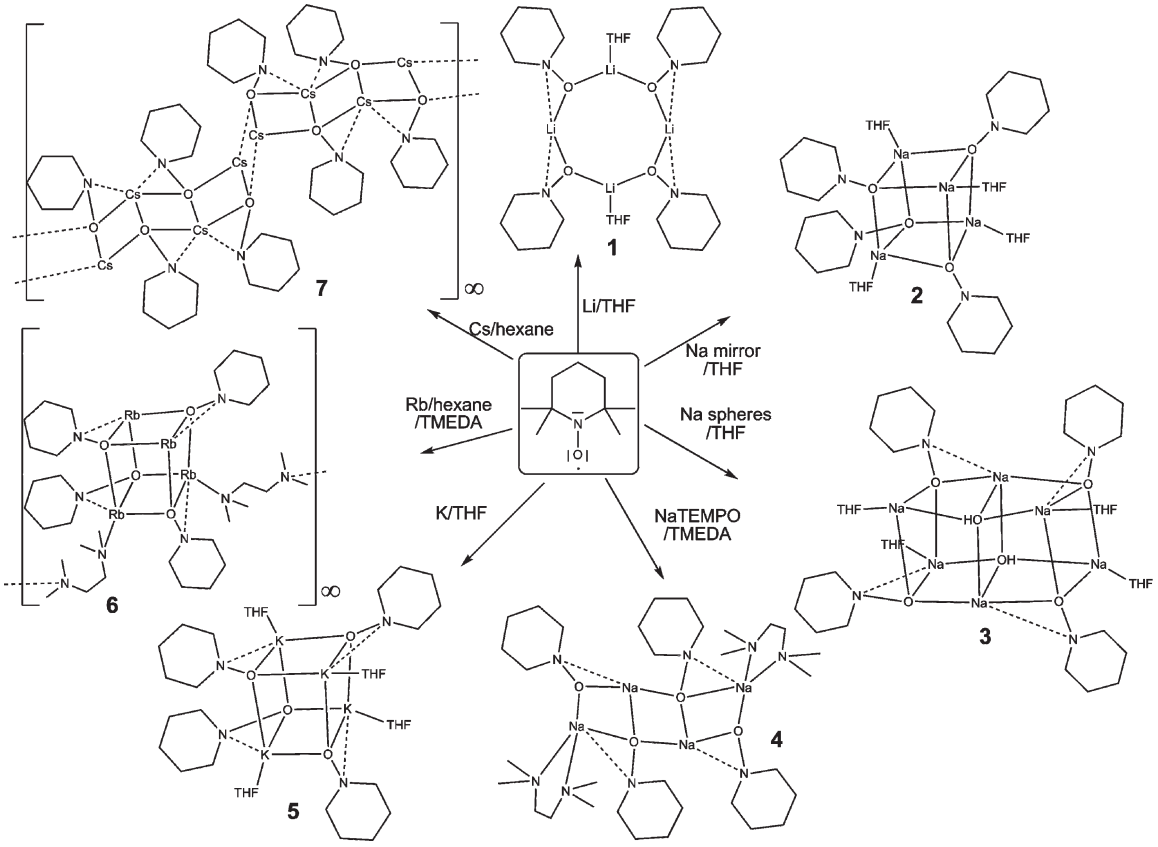

[a] For clarity, M−N_{TEMPO} bonds have been drawn as dotted lines, and Me groups have been omitted from the TEMPO units. In **6**, each Rb is coordinated to half a molecule of TMEDA.

Synthesis of $[Na_4^+(\mu_3\text{-}TEMPO^-)_2(\mu\text{-}TEMPO^-)_2(TMEDA)_2]$ (4). Freshly prepared Na^+TEMPO^- (0.36 g, 2 mmol) was suspended in hexane in a Schlenk tube. TMEDA (0.15 mL, 1 mmol) was added, and the mixture was stirred overnight. The subsequent mixture was filtered, and the red filtrate was concentrated by removal of some solvent in vacuo and placed in the freezer at −26 °C. A crop of colorless crystals was deposited after 24 h. Yield: 0.28 g, 59%. ^{1}H NMR (D_8-THF, 400 MHz, 300 K): δ 2.30 (CH_2, TMEDA, 4H, s), 2.15 (CH_3, TMEDA, 6H, s), 1.44 (β-H and γ-H, 6H, br s), 1.06 (CH_3, 12H, br s). ^{13}C NMR (D_8-THF, 100 MHz, 300 K): 58.9 (α-*C*), 58.5 (*C*H_2, TMEDA), 46.2 (*C*H_3, TMEDA), 41.2 (β-*C*), 18.7 (γ-*C*).

Synthesis of $[(THF)\cdot K^+(TEMPO^-)]_4$ (5). A Schlenk tube was charged with freshly cleaned elemental potassium (0.39 g, 10 mmol). THF (50 mL) and TEMPO (1.56 g, 10 mmol) were then added, and this orange-colored mixture was heated to melt the metal. On cooling to room temperature, small spheres of metal formed. This mixture was allowed to stir at ambient temperature for 48 h. The colorless solution was filtered, and approximately 50% of the solution was removed in vacuo. This solution was cooled to −20 °C for 24 h to precipitate a large crop of colorless crystals of **5** (0.56 g, 21%). ^{1}H NMR (D_8-THF, 400 MHz, 300 K): δ 3.61 (O*C*H_2, THF, 2H, s), 1.77 (*C*H_2, THF, 2H, s), 1.42 (β-H and γ-H, 6H, br s), 1.00 (CH_3, 12H, br s). ^{13}C NMR (D_8-THF, 100 MHz, 300 K): 68.2 (O*C*H_2, THF), 58.4 (α-*C*), 41.7 (β-*C*), 35.6 (*C*H_3), 26.4 (*C*H_2, THF), 18.7 (γ-*C*), 18.7 (*C*H_3).

Synthesis of $[(TMEDA)\cdot Rb_2^+(TEMPO^-)_2]_2$ (6). Rubidium metal (0.17 g, 2.0 mmol) was placed in a Schlenk tube with hexane (20 mL) along with TEMPO (0.32 g, 2.0 mmol). The mixture was gently heated to melt the rubidium and stirred for 2 h. During this time the metal dissolves, the dark orange color of the TEMPO fades, and a colorless precipitate appears. A vast excess of TMEDA (1.50 mL, 10.0 mmol) was introduced, and the solution was again gently heated until the precipitate dissolved. To aid crystal growth, the slightly cloudy solution was filtered, and most of the solvent removed in vacuo. At ambient temperature small cubic crystals were obtained (0.10 g, 17%).^{1}H NMR (D_8-THF, 400 MHz, 300 K): δ 2.30 (CH_2, TMEDA, 4H, s), 2.15 (CH_3, TMEDA, 6H, s), 1.42 (β-H and γ-H, 6H, br s), 1.00 (CH_3, 12H, br s). ^{13}C NMR (D_8-THF, 100 MHz, 300 K): 58.9 (α-*C*), 58.5 (*C*H_2, TMEDA), 46.2 (*C*H_3, TMEDA), 41.4 (β-*C*), 34.5 (*C*H_3), 18.9 (γ-*C*) 18.5 (*C*H_3).

Synthesis of $[Cs^+(TEMPO^-)]_\infty$ (7). A Schlenk tube was charged with elemental cesium (0.27 g, 2 mmol). THF (20 mL) and TEMPO (0.46 g, 3 mmol) were then added, and this orange-colored mixture was stirred at ambient temperature for 18 h. The resultant golden-colored solution was filtered, and approximately 50% of the solution was removed in vacuo. This solution was left at ambient temperature for 24 h to precipitate a crop of colorless crystals of **7** (0.19 g, 33%). ^{1}H NMR (D_8-THF, 400 MHz, 300 K): δ 1.43 (β-H and γ-H, 6H, br s), 0.99 (CH_3, 12H, br s). ^{13}C NMR (D_8-THF, 100 MHz, 300 K): 58.3 (α-*C*), 41.2 (β-*C*), 34.5 (*C*H_3), 19.2 (*C*H_3), 18.9 (γ-*C*).

Results

Syntheses. Scheme 2 outlines the syntheses of the alkali metal TEMPO complexes **1**−**7**. In general, the complexes are formed by the direct reaction of the alkali metal with an equimolar quantity of TEMPO in the respective solvent medium under a protective argon atmosphere. Formation of **1**−**7**, coinciding with the one-electron

reduction of the TEMPO radical to the $TEMPO^-$ anion (Scheme 1), is accompanied by the gradual loss of the initial vivid orange/red color as the solution is heated to reflux (or left stirring at ambient temperature for **7**). Our focus was on growing suitable crystalline complexes for X-ray crystallographic characterization rather than on optimizing product yields.

For **1**, the mixture of lithium metal and TEMPO in THF was heated to reflux for 100 h, and the salt precipitates from solution as a white powder. Additionally, colorless X-ray quality crystals (in a moderate to good yield) were obtained by cooling the mother liquor to −30 °C for 48 h. Both forms of **1** lose THF during the in vacuo filtration/isolation process and give the same analysis.

For **2**, a sodium mirror was prepared by melting freshly cleaned sodium metal in a Schlenk tube and heating it with a heat gun. After the addition of TEMPO and THF, the mixture was heated to reflux for 48 h. On cooling this solution to −20 °C, a crop of colorless crystals of **2** precipitated.

For **3**, in an effort to prepare a sodium mirror, sodium spheres were placed in a flame-dried Schlenk tube and melted using a heat gun. Because of the tarnished surface of the metallic spheres, the sodium mirror was of poor quality and presumably contaminated with oxygen-based species. After the addition of TEMPO and THF, the mixture was heated to reflux for 72 h. A red/orange to brown color change was noted. On cooling this solution to −20 °C for 24 h, a crop of colorless crystals (low yield) of **3** precipitated. Unfortunately, because of the rather fortuitous nature of this synthesis, **3** could not be obtained reproducibly.

For **4**, TMEDA was added to a suspension of freshly prepared Na^+TEMPO^- (a powder which was prepared by reacting Na with TEMPO in hexane) in hexane solution. After stirring this mixture overnight and cooling the solution to −26 °C, crystals of **4** precipitated in moderate yield.

For **5**, a potassium mirror was prepared by melting freshly cut K metal in a Schlenk tube. THF and TEMPO were added to the metal. Dissolution of the metallic K and complete loss of color was observed after 48 h of heating the THF solution to reflux. Cooling the solution to −20 °C for 48 h yielded X-ray quality crystals of **5** in moderate yield.

For **6**, rubidium metal and TEMPO were combined in hexane solution. The mixture only required gentle heating to melt the metal, and after stirring for 2 h the metal dissolved and the dark orange color of the TEMPO faded. A colorless precipitate then started to appear, which was redissolved by the addition of excess TMEDA and gentle heating. Small cubic crystals formed at ambient temperature in low yield and were found to be extremely soluble in the solvent medium.

For **7**, molten Cs was added to a Schlenk tube via a pipet. The hexane solution of the metal and TEMPO were allowed to stir at ambient temperature for 18 h. Over a period of 10 days, colorless needle-like crystals deposited from the solution.

Solid-State Structures. The molecular structure of **1** and its key structural parameters are shown in Figure 1. Within this structure, there are 0.5 mol equiv of THF to each Li^+TEMPO^- contacted ion pair arranged in an eight-membered $(LiO)_4$ ring (Figure 1).

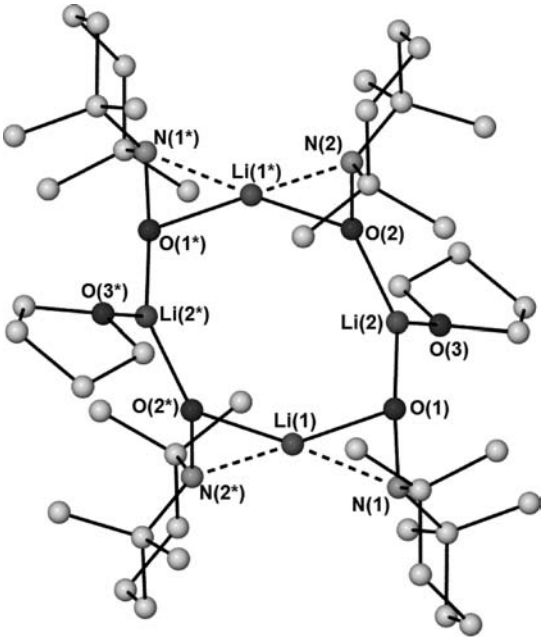

Figure 1. Molecular structure of $(THF)_2 \cdot [Li(TEMPO)]_4$ **1**. Key dimensions (Å and deg): Li(1)−O(1) 1.885(3), Li(1)−O(2*) 1.857(3), Li(2)−O(1) 1.784(3), Li(2)−O(2) 1.824(3), Li(1)−N(1) 2.062(3), Li(1)−N(2*) 2.050(3), O(1)−N(1) 1.433(2), O(2)−N(2) 1.441(2), O(1)−Li(1)−N(1) 42.29(7), O(2)−Li(1*)−N(2) 42.93(7), Li(1)−O(1)−N(1) 75.46(11), Li(1*)−O(2)−N(2) 75.68(11), Li(1)−N(1)−O(1) 62.25(10), Li(1*)−N(2)−O(2) 61.38(10), O(1)−Li(2)−O(3) 119.24(15), O(2)−Li(2)−O(3) 107.51(14). Here and in the text the symmetry transformations used to generate equivalent atoms: * $-x+1, -y+1, -z$.

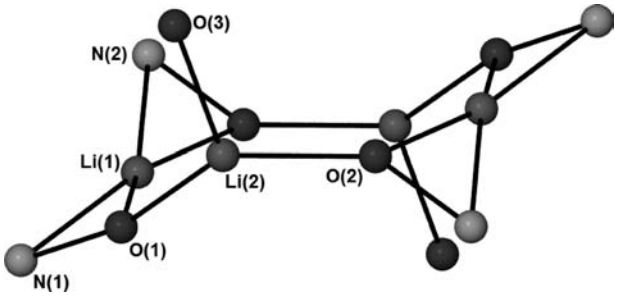

Figure 2. Metal heteroatom framework of **1**. All C atoms have been removed for clarity.

This ring is non-planar and composed of three separate planes: Li(2)···O(2*)−Li(1)−O(1), O(2)···Li(2*)−O(2*)···Li(2) and Li(1*)−O(1*)−Li(2*)···O(2) (Figure 2). Possessing C_i symmetry, the structure can be described as pseudotetrameric: four-coordinate Li(1) is a novel *spiro* center for two Li−O−N triangles, while three-coordinate Li(2) carries a THF molecule. To the best of our knowledge only two lithium hydroxylamine[43] structures are available for comparison, namely, the benzylamine $[\{LiON(CH_2Ph)_2\}_6]$[44] and the silylamine $[\{LiON(SiMe_2Bu^t)_2 \cdot THF\}_2]$.[45] Incidentally, unlike **1** (which was

(43) For early studies on lithium hydroxylamines see: West, R.; Boudjouk, P. *J. Am. Chem. Soc.* **1973**, *95*, 3987–3994.

(44) Armstrong, D. R.; Clegg, W.; Hodgson, S. M.; Snaith, R.; Wheatley, A. E. H. *J. Organomet. Chem.* **1998**, *550*, 233–240.

(45) Diedrich, F.; Klingebiel, U.; Schäfer, M. *J. Organomet. Chem.* **1999**, *588*, 242–246.

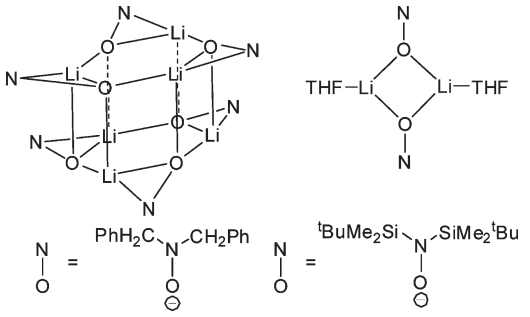

Figure 3. Structural formulas of the lithium hydroxylamines, [{LiON-$(CH_2Ph)_2\}_6$][44] and solvated [{LiON($SiMe_2Bu^t)_2$.THF}$_2$].[45]

prepared by metal-induced reduction of TEMPO) the former was prepared by a common metalation strategy, while the latter involved the metalation of $Bu^tMe_2SiON(H)SiMe_2Bu^t$ followed by an O to N silyl group migration.

Structurally, both deviate markedly from each other and from that of **1**. In contrast to the unique architecture of **1**, the hexameric [a stack of two $(LiO)_3$ rings] and dimeric [a discrete $(LiO)_2$ planar ring] cores of unsolvated [{LiON$(CH_2Ph)_2\}_6$][44] and solvated [{(THF)·LiON($SiMe_2Bu^t)_2\}_2$],[45] respectively, are commonly encountered in lithium organoelement chemistry (Figure 3).[46,47] Their N−O functionalities exhibit N/O chelation in the benzylamine [confined to one LiON chelate per Li as opposed to two for Li(1) in **1**] and O coordination (with no Li−N bonding) in the silylamine.

Double triangular chelation of Li(1) in **1** gives a four-coordinate geometry far removed from tetrahedral as evidenced by the sharp N−O bite angles [mean, 42.61°, cf., 41.02° in [{LiON$(CH_2Ph)_2\}_6$].[44] The two triangles are twisted at an angle of 52.7(1)° relative to each other. A concomitant effect of the chelation is to widen the $(LiO)_4$ ring at Li(1) [bond angle, 142.34(17)°; cf., 132.17-(17)° at Li(2)]; this is accompanied by a large angular disparity at the O atoms [Li(1)O(1)Li(2), 105.90(13)°; Li-(1)O(2*)Li(2*), 133.96(14)°]. Non-chelated Li(2) enjoys a more usual distorted trigonal planar geometry (sum of bond angles, 358.92°). A combination of chelation and coordination number effects encourages long [relative to those of Li(2)] Li(1)−O(1)/Li(1)−O(2*) bond lengths [mean, 1.871 Å; cf., 1.943 Å for the corresponding bonds in [{LiON$(CH_2Ph)_2\}_6$],[44] while the modest difference between the non-chelated Li(2)−O(1)/Li(2)−O(2) bond lengths [1.784(3)/1.824(3) Å] reflects the strained asymmetrical nature of the gross molecule. The longest Li−O bond in **1** at 2.008(3) Å is that [Li(2)−O(3)] involving THF. Corresponding values for the Li atoms in [{(THF)· LiON($SiMe_2Bu^t)_2\}_2$][45] which display an identical coordination to that of Li(2) are of a similar magnitude [i.e., range of Li-μ-O, 1.826−1.846 Å; Li−O-(THF), 1.957(5) Å]. There is a telling difference in the Li−N bond lengths in **1** (mean, 2.056 Å) compared to those in [{LiON$(CH_2Ph)_2\}_6$][44] (mean, 2.131 Å); but significantly their N−O bond lengths are essentially

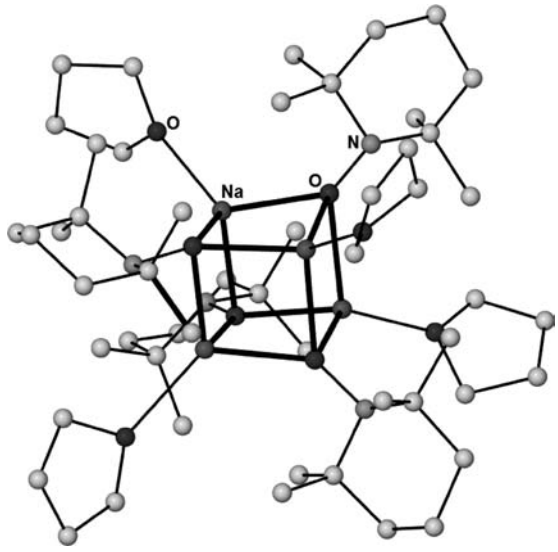

Figure 4. Molecular structure of [(THF)·Na(TEMPO)]$_4$ **2**.

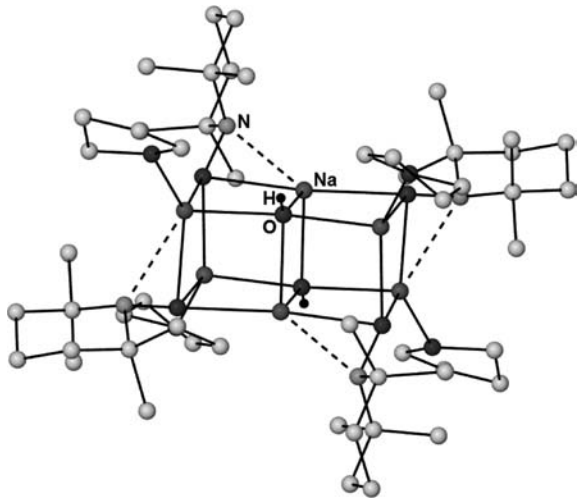

Figure 5. Molecular structure of [$(THF)_2$·$Na_3(TEMPO)_2(OH)]_2$ **3**.

equivalent (mean, 1.437 and 1.438 Å, respectively). Overall, therefore, the LiON chelates in **1** have contracted relative to those in [{LiON$(CH_2Ph)_2\}_6$],[44] but only on two sides (Li−O/Li−N); with the N−O side seemingly insensitive to changes in aggregation, the amido substituent or the local coordination environment.

The molecular structures of **2** and **3** are shown in Figures 4 and 5, respectively. The X-ray data for **2** and **3** are both suboptimal. This precludes a detailed discussion of geometric parameters; however, in both cases the atom connectivities are unequivocal. To the best of our knowledge, these structures represent the first structurally characterized sodium hydroxylamine structures. Complex **2** crystallizes in the monoclinic system, space group $P2_1/n$. Although both complexes **1** and **2** are tetranuclear, their structures differ markedly from one another. The central core of **2** (Figure 4) consists of interpenetrating tetrahedra of Na and O_{TEMPO} atoms resulting in the formation of a distorted cubane—a motif which is commonly encountered in sodium

(46) Mulvey, R. E. *Chem. Soc. Rev.* **1991**, *20*, 167–209.
(47) Gregory, K.; Schleyer, P. V.; Snaith, R. *Adv. Inorg. Chem.* **1991**, *37*, 47–142.

alkoxide/aryloxide or siloxide chemistry.[48−70] Each Na atom coordinates to three anionic O_{TEMPO} centers, and the metal's coordination sphere is completed by complexation to a THF molecule. In contrast to **1**, there appears to be no significant M−N bonding in **2**, which may be attributed to the relatively more compact nature of the M_4O_4 core in **2** and the fact that the metal to THF ratio in **2** is 1:1 (cf., 2:1 for **1**).

Complex **3** crystallizes in the triclinic system, space group $P\bar{1}$. It exists as a hexanuclear face-sharing bis-cubane in the solid state (Figure 5). The central core of **3** consists of two outer Na_2O_2 rings, where O belongs to the $TEMPO^-$. These two rings are separated by a third Na_2O_2 ring; however, this time the O atoms belong to hydroxyl groups. Presumably because of the presence of NaOH (or H_2O) during the preparation of **3**, it appears that 2 equivs of NaOH have been incorporated into the structure of **2** altering it from a discrete cube to the bis-cube. Therefore **3** can be considered as a mixed aggregate of $[(THF)\cdot Na(TEMPO)]_2$ and $(NaOH)_2$. Several Na- and O-containing bis-cubane structures have been reported previously;[49,60,71,72] however, **3** appears to be the only heteroleptic example.

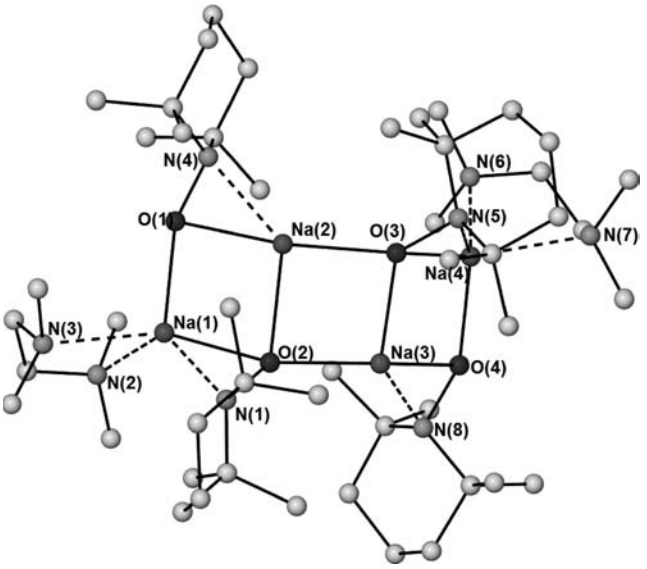

Figure 6. Asymmetric unit of **4**. Key dimensions (Å and deg): Na(1)−O(1) 2.1992(12), Na(1)−O(2) 2.3107(11), Na(1)−N(1) 2.4705(13), Na(1)−N(2) 2.6986(15), Na(1)−N(3) 2.4726(14), Na(2)−O(1) 2.3059(11), Na(2)−O(2) 2.3443(11), Na(2)−O(3) 2.2673(11), Na(2)−N(4) 2.4287(14), Na(3)−O(2) 2.2446(11), Na(3)−O(3) 2.3059(11), Na(3)−O(4) 2.2919(12), Na(3)−N(8) 2.3815(13), Na(4)−O(3) 2.4399(12), Na(4)−O(4) 2.1941(12), Na(4)−N(5) 2.4347(13), Na(4)−N(6) 2.8080(15), Na(4)−N(7) 2.5299(14), O(1)−N(4) 1.4345(15), O(2)−N(1) 1.4447(14), O(3)−N(5) 1.4436(14), O(4)−N(8) 1.4376(15), O(1)−Na(1)−O(2) 99.92(4), O(1)−Na(1)−N(1) 120.14(5), O(1)−Na(1)−N(2) 109.43(5), O(1)−Na(1)−N(3) 101.24(5), O(2)−Na(1)−N(1) 34.97(3), O(2)−Na(1)−N(2) 130.19(5) O(2)−Na(1)−N(3) 140,71(5), N(1)−Na(1)−N(2) 129.47(5), N(1)−Na(1)−N(3) 105.95-(5), N(2)−Na(1)−N(3) 71.49(5), O(1)−Na(2)−O(2) 95.91(4), O(1)−Na-(2)−O(3) 164.94(5), O(1)−Na(2)−N(4) 35.15(4), O(2)−Na(2)−O(3) 91.51(4), O(2)−Na(2)−N(4) 130.55(4), O(3)−Na(2)−N(4) 134.23(5), O-(2)−Na(3)−O(3) 93.10(4), O(2)−Na(3)−O(4) 146.76(5), O(2)−Na(3)−N(8) 122.15(4), O(3)−Na(3)−O(4) 98.20(4), O(3)−Na(3)−N(8) 133.46(4), O(4)−Na(3)−N(8) 35.76(4), O(3)−Na(4)−O(4) 97.04(4), O(3)−Na(1)−N(5) 34.45(4), O(3)−Na(4)−N(6) 129.86(4), O(3)−Na(4)−N(7) 143.77-(5), O(4)−Na(4)−N(5) 118.43(5), O(4)−Na(4)−N(6) 112.72(5), O(4)−Na(4)−N(7) 101.31(5), N(5)−Na(4)−N(6), 127.41(5), N(5)−Na(4)−N(7) 109.74(5), N(6)−Na(4)−N(7) 69.79(4), Na(1)−O(1)−Na(2) 83.70(4), Na(1)−O(2)−Na(2) 80.47(4), Na(2)−O(2)−Na(3) 84.03(4), Na(2)−O-(3)−Na(3) 84.40(4), Na(3)−O(3)−Na(4), 79.27(4), Na(3)−O(4)−Na(4) 84.91(4).

The molecular structure of **4** and key dimensions are shown in Figure 6. Complex **4** crystallizes in the triclinic system, space group $P\bar{1}$, and exists as a discrete tetranuclear pseudodimer which adopts a ladder-like conformation. The Na atoms which occupy positions in the outer rungs [Na(1) and Na(4)] are five-coordinate, coordinated to one μ_2-O, one μ_3-O, one N_{TEMPO}, and two N_{TMEDA} atoms. Those occupying the central rungs [Na-(2) and Na(3)] adopt a highly distorted tetrahedral geometry [angles (mean), 108.72 and 104.91°, respectively]. The mean acute O−Na−N_{TEMPO} and TMEDA bite angles are 35.08 and 70.64°, respectively. Turning to the bond distances in **4**, the shortest Na−O bonds are those belonging to the end rungs of the ladder [2.1992(12) and 2.1941(12) Å for Na(1)−O(1) and Na(4)−O(4)]. The remaining Na−O bonds range in length from 2.2446(11) to 2.4399(12) Å. Ladder motifs are commonly observed in the organometallic chemistry of the alkali metals.[46,47,73]

(48) Clegg, W.; Davidson, M. G.; Graham, D. V.; Griffen, G.; Jones, M. D.; Kennedy, A. R.; O'Hara, C. T.; Russo, L.; Thomson, C. M. *Dalton Trans.* **2008**, 1295–1301.
(49) Kuckmann, T. I.; Bolte, M.; Wagner, M.; Lerner, H. W. *Z. Anorg. Allg. Chem.* **2007**, *633*, 290–297.
(50) Deacon, G. B.; Feng, T. C.; Hockless, D. C. R.; Junk, P. C.; Skelton, B. W.; Smith, M. K.; White, A. H. *Inorg. Chim. Acta* **2007**, *360*, 1364–1369.
(51) Geier, J.; Ruegger, H.; Grutzmacher, H. *Dalton Trans.* **2006**, 129–136.
(52) Cole, M. L.; Junk, P. C.; Proctor, K. M.; Scott, J. L.; Strauss, C. R. *Dalton Trans.* **2006**, 3338–3349.
(53) Muller, G.; Schätzle, T. *Z. Naturforsch., B: Chem. Sci.* **2004**, *59*, 1400–1410.
(54) Fischer, R.; Görls, H.; Walther, D. *Z. Anorg. Allg. Chem.* **2004**, *630*, 1387–1394.
(55) Lerner, H. W.; Scholz, S.; Bolte, M. *Organometallics* **2002**, *21*, 3827–3830.
(56) Sobota, P.; Klimowicz, M.; Utko, J.; Jerzykiewicz, L. B. *New J. Chem.* **2000**, *24*, 523–526.
(57) Hou, Z. M.; Jia, X. S.; Fujita, A.; Tezuka, H.; Yamazaki, H.; Wakatsuki, Y. *Chem.—Eur. J.* **2000**, *6*, 2994–3005.
(58) Chi, Y.; Ranjan, S.; Chung, P. W.; Liu, C. S.; Peng, S. M.; Lee, G. H. *J. Chem. Soc., Dalton Trans.* **2000**, 343–347.
(59) Czado, W.; Muller, U. *Z. Kristallogr. − New Cryst. Struct.* **1999**, *214*, 63–64.
(60) Kunert, M.; Dinjus, E.; Nauck, M.; Sieler, J. *Chem. Ber.* **1997**, *130*, 1461–1465.
(61) Mommertz, A.; Dehnicke, K.; Magull, J. *Z. Nat. Sect. B* **1996**, *51*, 1583–1586.
(62) Hou, Z. M.; Fujita, A.; Yamazaki, H.; Wakatsuki, Y. *J. Am. Chem. Soc.* **1996**, *118*, 2503–2504.
(63) Samuels, J. A.; Folting, K.; Huffman, J. C.; Caulton, K. G. *Chem. Mater.* **1995**, *7*, 929–935.
(64) Fryzuk, M. D.; Gao, X. L.; Rettig, S. J. *Can. J. Chem.* **1995**, *73*, 1175–1180.
(65) Walther, D.; Ritter, U.; Gessler, S.; Sieler, J.; Kunert, M. *Z. Anorg. Allg. Chem.* **1994**, *620*, 101–106.
(66) Vanderschaaf, P. A.; Jastrzebski, J.; Hogerheide, M. P.; Smeets, W. J. J.; Spek, A. L.; Boersma, J.; Vankoten, G. *Inorg. Chem.* **1993**, *32*, 4111–4118.
(67) Samuels, J. A.; Lobkovsky, E. B.; Streib, W. E.; Folting, K.; Huffman, J. C.; Zwanziger, J. W.; Caulton, K. G. *J. Am. Chem. Soc.* **1993**, *115*, 5093–5104.
(68) Evans, W. J.; Golden, R. E.; Ziller, J. W. *Inorg. Chem.* **1993**, *32*, 3041–3051.
(69) Solari, E.; Deangelis, S.; Floriani, C.; Chiesivilla, A.; Rizzoli, C. *J. Chem. Soc., Dalton Trans.* **1991**, 2471–2476.
(70) Hughes, D. L.; Wingfield, J. N. *J. Chem. Soc., Chem. Commun.* **1984**, 408–409.
(71) MacDougall, D. J.; Noll, B. C.; Henderson, K. W. *Inorg. Chem.* **2005**, *44*, 1181–1183.
(72) Hogerheide, M. P.; Ringelberg, S. N.; Janssen, M. D.; Boersma, J.; Spek, A. L.; van Koten, G. *Inorg. Chem.* **1996**, *35*, 1195–1200.
(73) Weiss, E. *Angew. Chem., Int. Ed. Engl.* **1993**, *32*, 1501–1523.

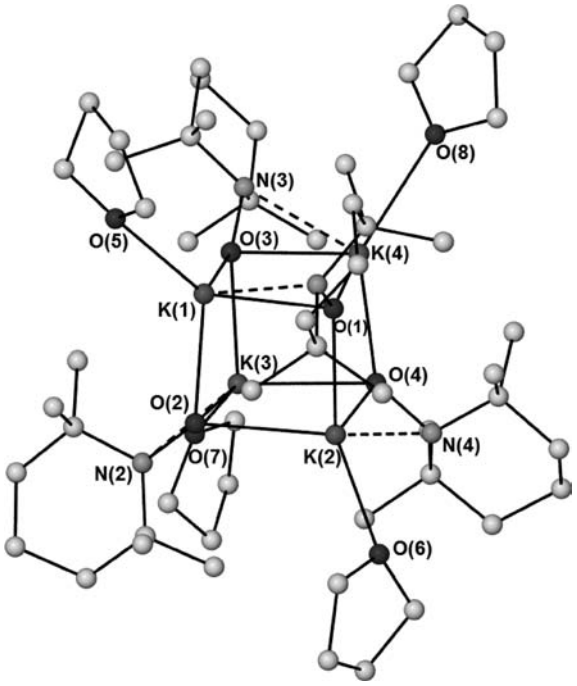

Figure 7. Molecular structure of $[(THF)\cdot K(TEMPO)]_4$ **5**. Key dimensions (Å and deg): K(1)−O(1) 2.5750(19), K(1)−O(2) 2.6370(18), K(1)−O(3) 2.7182(18), K(2)−O(1) 2.6436(18), K(2)−O(2) 2.7393(18), K(2)−O(4) 2.5615(17), K(2)−O(6) 2.7110(19), K(3)−O(2) 2.5741(18), K(3)−O(3) 2.6114(17), K(3)−O(4) 2.7114(18), K(3)−O(7) 2.710(2), K(4)−O(1) 2.6896(17), K(4)−O(3) 2.5748(18), K(4)−O(4) 2.6514(17), K(4)−O(8) 2.718(2), K(1)−N(1) 2.938(2), K(2)−N(4) 2.853(2), K(3)−N(2) 2.889(2), K(4)−N(3) 2.930(2), O(1)−N(1) 1.440(3), O(2)−N(2) 1.439(3), O(3)−N(3) 1.441(2), O(4)−N(4) 1.439(3), O(1)−K(1)−O(2) 92.69(6), O(1)−K(1)−O(3) 94.93(5), O(1)−K(1)−O(5) 121.3(3), O(1)−K(1)−O(5A) 116.13(19), O(1)−K(1)−N(1) 29.35(5), O(2)−K(1)−O(3) 87.95(5), O(2)−K(1)−O(5) 130.9(2), O(2)−K(1)−O(5A) 139.03(19), O(2)−K(1)−N(1) 109.65(6), O(3)−K(1)−O(5) 119.5(3), O(3)−K(1)−O(5A) 115.82(19), O(3)−K(1)−N(1) 118.26(6), O(5)−K(1)−N(1) 92.8(3), O(5A)−K(1)−N(1) 88.75(19), O(1)−K(2)−O(2) 88.93(5), O(1)−K(2)−O(4) 90.85(5), O(1)−K(2)−O(6) 126.08(6), O(1)−K(2)−N(4) 108.52(6), O(2)−K(2)−O(4) 96.94(5), O(2)−K(2)−O(6) 116.40(6), O(2)−K(2)−N(4) 120.48(6), O(4)−K(2)−O(6) 128.01(6), O(4)−K(2)−N(4) 30.23(5), O(6)−K(2)−N(4) 98.30-(6), O(2)−K(3)−O(3) 91.64(5), O(2)−K(3)−O(4) 97.34(5), O(2)−K(3)−O(7) 126.34(6), O(2)−K(3)−N(2) 29.83(5), O(3)−K(3)−O(4) 89.50(5), O(3)−K(3)−O(7) 124.10(6), O(3)−K(3)−N(2) 108.84(6), O(4)−K(3)−O(7) 118.94(6), O(4)−K(3)−N(2) 120.48(6), O(7)−K(3)−N(2) 96.79(6), O(1)−K(4)−O(3) 95.63(6), O(1)−K(4)−O(4) 89.42(4), O(1)−K(4)−O(8) 116.48(6), O(1)−K(4)−N(3) 118.49(6), O(3)−K(4)−O(4) 91.63(6), O(3)−K(4)−O(8) 119.89(6), O(3)−K(4)−N(3) 29.46(5), O(4)−K(4)−O(8) 135.40(6), O(4)−K(4)−N(3) 109.42(6), O(8)−K(4)−N(3) 91.65(6).

The ladder core of **4** comprises three Na_2O_2 rhombi; the outermost rings are essentially planar, while the central ring deviates significantly from planarity [sum of endocyclic angles for Na(1)−O(1)−Na(2)−O(2), O(2)−Na(2)−O(3)−Na(3), and Na(3)−O(3)−Na(4)−O(4) rings are 360, 353.04 and 359.42° respectively]. The dihedral angles between planes Na(1)−O(1)−Na(2)−O(2) and O(2)−Na(2)−O(3)−Na(3), and O(2)−Na(2)−O(3)−Na(3) and Na(3)−O(3)−Na(4)−O(4) are 154.44(3)° and 133.92(3)°, respectively, resulting in the ladder adopting a cisoidal conformation.

The molecular structure of **5** and key dimensions are shown in Figure 7. Complex **5** crystallizes in the triclinic system, space group $P\bar{1}$, and adopts a tetranuclear distorted cubane structure which is essentially isostructural to **2**; however, the dimensions of this structure can be discussed in more detail as the only element of disorder

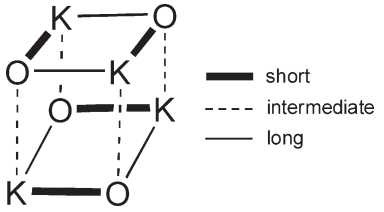

Figure 8. Three categories of $K-O_{TEMPO}$ distance in **5**.

involves the THF molecule attached to K(1). Each corner-positioned K atom is coordinated by three μ_3-O_{TEMPO} atoms and a THF molecule. The metal's stabilization is further supplemented by bonding to a N_{TEMPO} atom (in contrast to the situation observed in **2**). As a result, each five-coordinate K center has one highly acute N−K−O angle [range, 29.35(5)−30.23(5)°]. Within the K_4O_4 cube, the $K-O_{TEMPO}$ bond distances vary considerably, in the range 2.5748(18)−2.7393(18) Å. There are three distinct $K-O_{TEMPO}$ bond distance regions in the molecule: short [2.5615(17)−2.5750(19) Å]; intermediate [2.6114(17)−2.6514(17) Å]; and long [2.6896(17)−2.7393-(18) Å] (Figure 8). The short and long bonds alternate in two K_2O_2 rings, and these are subsequently laterally connected (stacked) via the intermediate bonds (Figure 8). This fits the ring-laddering principle conceived by Snaith.[47] The four shortest $K-O_{TEMPO}$ bonds [K(1)−O-(1), K(2)−O(4), K(3)−O(2) and K(4)−O(3)] are presumably strengthened because of the additional stabilization to the metal from the N adjacent to the respective O [i.e., the presence of K(1)−N(1), K(2)−N(4), K(3)−N(2), and K(4)−N(3) bonds]. The N−O bonds in **5** are again indicative of an anionic TEMPO ligand and are identical to those in **1** and in the previously mentioned lithium hydroxylamines.[44,45] In 2008, Mitzel et al. documented the synthesis (via deprotonation of a hydroxylamine with potassium hydride) and structure of three potassium hydroxylamine complexes.[74] Two of these complexes, $[(Me_2NOK)(Me_2NOH)]_\infty$ and $[(^iPr_2NOK)(^iPr_2NOH)\text{-}(THF)]_\infty$, are polymeric. The third $[\{(C_6H_5CH_2)_2NOK\}_6\text{-}(THF)_4]$ is molecular, and resembles the bis-cubane structural framework of sodium-containing **3**. The range of $K-O_{TEMPO}$ bond lengths in **5** [2.5748(18)−2.7393(18) Å] is similar to that in $[\{(C_6H_5CH_2)_2NOK\}_6(THF)_4]$ [2.562(2)−2.812(2) Å]. Also the mean K−N bond in **5** (mean distance, 2.903 Å) bears a close resemblance to that in $[\{(C_6H_5\text{-}CH_2)_2NOK\}_6(THF)_4]$ (2.861 Å). In addition, the key bond angles in the complexes are similar, including the mean O−K−N angle [29.72° in **5** and 29.57° in $[\{(C_6H_5CH_2)_2\text{-}NOK\}_6(THF)_4]$. Mitzel also published the synthesis and structure of another potassium hydroxylamine-containing bis-cubane $[(Me_3SiO)_4\{(Me_3Si)_2NO\}_2K_6]$[75] in 2008. This complex is a heteroleptic example which contains silylhydroxylamide and silanolate ligands. It is formed by a combination of deprotonations, N−O bond cleavages and 1,2-shifts of a trimethylsilyl group after treating *N,O*-bis(trimethylsilyl)hydroxylamine with potassium hydride.

(74) Venugopal, A.; Berger, R. J. F.; Willner, A.; Pape, T.; Mitzel, N. W. *Inorg. Chem.* **2008**, *47*, 4506–4512.
(75) Venugopal, A.; Willner, A.; Mitzel, N. W. *Z. Naturforsch.* **2008**, *63b*, 339–341.

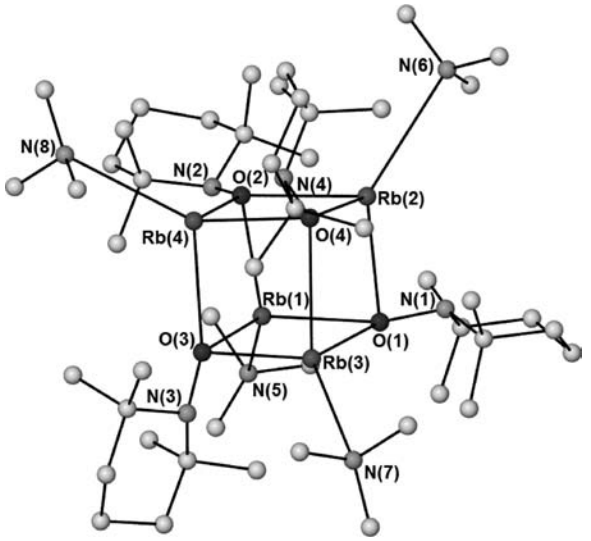

Figure 9. Asymmetric unit of **6**. For clarity Rb−N_{TEMPO} bonds have been omitted. Key dimensions (Å and deg): Rb(1)−O(1) 2.9171(14), Rb(1)−O(2) 2.6756(12), Rb(1)−O(3) 2.8196(15), Rb(1)−N(2) 2.9892(19), Rb(1)−N(5) 3.337(2), Rb(2)−O(1) 2.6926(16), Rb(2)−O(2) 2.9081(14), Rb(2)−O(4) 2.7599(15), Rb(2)−N(1) 2.9573(18), Rb(2)−N(6) 3.285(2), Rb(3)−O(1) 2.7587(15), Rb(3)−O(3) 2.6710(14), Rb(3)−O(4) 3.0180(16), Rb(3)−N(3) 2.9902(18), Rb(3)−N(7) 3.1825(18), Rb(4)−O(2) 2.7700(14), Rb(4)−O(3) 2.8896(16), Rb(4)−O(4) 2.6881(14), Rb(4)−N(4) 2.9808(19), Rb(4)−N(8) 3.2567(18), N(1)−O(1) 1.437(2), N(2)−O(2) 1.440(2), N(3)−O(3) 1.438(2), N(4)−O(4) 1.438(2). O(1)−Rb(1)−O(2) 92.98(4), O(1)−Rb(1)−O(3) 86.39(4), O(1)−Rb(1)−N(5) 122.36(5), O(2)−Rb(1)−O(3) 88.17(4), O(2)−Rb(1)−N(5) 124.76(5), O(3)−Rb(1)−N(5) 130.47(5), O(1)−Rb(2)−O(2) 92.83(5), O(1)−Rb(2)−O(4) 89.58(5), O(1)−Rb(2)−N(6) 136.34(5), O(2)−Rb(2)−O(4) 87.19(4), O(2)−Rb(2)−N(6) 111.82(4), O(4)−Rb(2)−N(6) 125.57(5), O(1)−Rb(3)−O(3) 92.64(4), O(1)−Rb(3)−O(4) 83.24(4), O(1)−Rb(3)−N(7) 126.48(5), O(3)−Rb(3)−O(4) 91.86(4), O(3)−Rb(3)−N(7) 127.63(5), O(4)−Rb(3)−N(7) 122.52(5), O(2)−Rb(4)−O(3) 85.00(4), O(2)−Rb(4)−O(4) 91.49(4), O(2)−Rb(4)−N(8) 121.84(5), O(3)−Rb(4)−O(4) 94.39(4), O(3)−Rb(4)−N(8) 123.93(5), O(4)−Rb(4)−N(8) 128.46(5).

The asymmetric unit of the crystal structure of **6** and key dimensions are shown in Figure 9. Complex **6** crystallizes in the monoclinic system, space group $P21/c$. Akin to **2** and **5**, the asymmetric unit of Rb-containing **6** adopts a tetranuclear distorted cubane structure; however, because of the inclusion of TMEDA, a three-dimensional polymeric array of cubane units is observed (Figure 10). In the asymmetric unit a half molecule of TMEDA is coordinated to each Rb. In general, TMEDA normally coordinates terminally (in a η^2-fashion) to an alkali metal, but perhaps counterintuitively, in the coordination chemistry of the larger Rb center, it appears that the monodentate bridging binding mode is highly prevalent. To the best of our knowledge there are only two known X-ray characterized examples of Rb complexes which coordinate TMEDA: first, the polymeric heterobimetallic mixed alkoxide/peroxide $[\{(LiO^tBu)_5(RbO^tBu)_4(Li_2O_2)\cdot(\mu\text{-TMEDA})_2\}_\infty]$; and second, the rubidium silylphosphide $[Rb\{P(H)Si^tBu_3\}\cdot(TMEDA)\cdot(\mu\text{-TMEDA})_{0.5}]_2$. In the former complex, akin to **6**, only the monodentate TMEDA binding mode is observed; but, in the latter example, both TMEDA binding modes, bridging and terminal, are exhibited. The Rb centers are crystallographically distinct and are all formally five-coordinate. Each Rb atom bonds to three μ_3-O_{TEMPO} centers, to one N atom of a TMEDA ligand and a N_{TEMPO} atom. The O−Rb−O bond angles vary from 83.24(4)−94.39(4)°

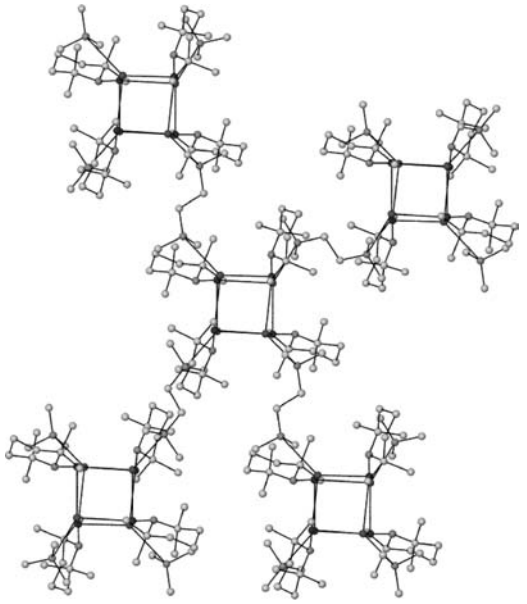

Figure 10. Polymeric array of $[(TMEDA)_2\cdot\{Rb(TEMPO^-)\}_4]$ units.

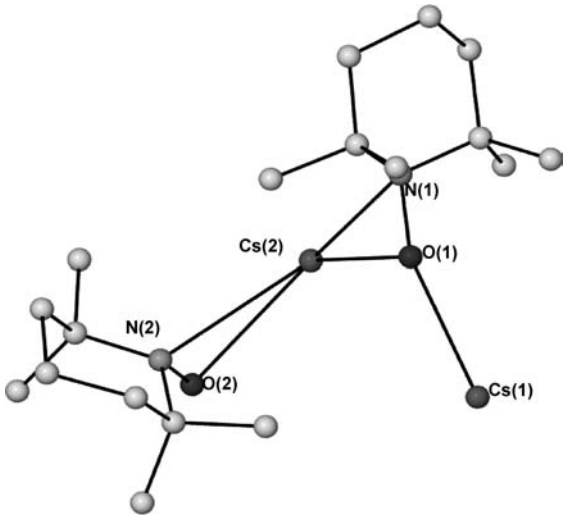

Figure 11. Asymmetric unit of **7**.

(consistent with a distorted cubane framework). The O−Rb−N_{TMEDA} angles [except for O(2)−Rb(2)−N(6), 111.82(4)°] are significantly wider than 109.5° [O−Rb−N range, 121.84(5)−136.34(5)°]. Turning to bond distances, the Rb−O bond distances vary considerably throughout the distorted cubane. Each of the three Rb−O bonds associated with a particular metal center can be classed as short, intermediate, or long. For instance, focusing on Rb(1), the distances of Rb(1)−O(1), Rb(1)−O(2), and Rb(1)−O(3) are 2.9171(14) (long), 2.6756(12) (short), and 2.8196(15) (intermediate), respectively. The shortest Rb−N bonds in **6** are the Rb−N_{TEMPO} bonds (mean distance, 2.979 Å) while the Rb−N_{TMEDA} bonds are almost 10% longer (mean distance, 3.265 Å). This latter distance indicates that the cubane units are only weakly held together by TMEDA in the extended structure.

The asymmetric unit of **7** is shown in Figure 11, while its extended structure and key dimensions are given in Figure 12. Complex **7** crystallizes in the monoclinic system, space group $C2/c$ and is polymeric in the solid

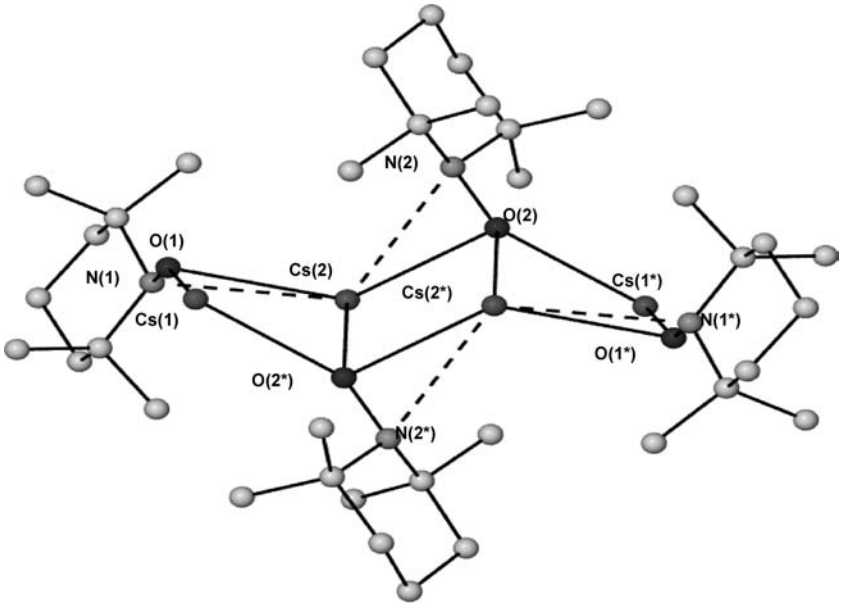

Figure 12. Repeating tetranuclear ladder motif of **7**. Key dimensions (Å and deg): Cs(1)−O(1) 2.713(2), Cs(1)−O(2*) 2.754(2), Cs(2)−O(1) 2.952(2), Cs(2)−O(2) 3.436(2), Cs(2)−O(2*) 2.963(2), Cs(2)−N(1) 3.133(3), Cs(2)−N(2) 3.089(2), N(1)−O(1) 1.440(3), N(2)−O(2) 1.435(3). O(1)−Cs(1)−O(2*) 99.76(7), O(1)−Cs(2)−O(2*) 81.39(5), O(1)−Cs(2)−N(1) 27.17(6), O(1)−Cs(2)−O(2) 123.36(6), O(1)−Cs(2)−N(2) 106.19(6), O(2*)−Cs(2)−N(1) 102.68-(5), O(2)−Cs(2)−O(2*) 80.86(6), O(2*)−Cs(2)−N(2) 98.70(6), O(2)−Cs(2)−N(1) 143.51(6), O(2)−Cs(2)−N(2) 27.33(6), N(1)−Cs(2)−N(2) 118.72(6), Cs(1)−O(1)−Cs(2) 92.39(6), N(1)−O(1)−Cs(1) 155.87(17), N(1)−O(1)−Cs(2) 83.43(14), Cs(1)−O(2*)−Cs(2) 81.94(5), Cs(1)−O(2*)−Cs(2*) 112.15(7), Cs(1)−O(1)−N(1) 143.74(17), Cs(2)−O(2*)−Cs(2*) 99.14(6), Cs(2)−O(2*)−N(2*) 130.80(15), Cs(2*)−O(2*)−N(2*) 81.22(13).

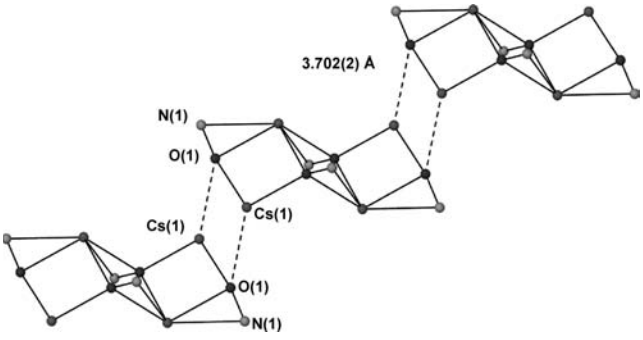

Figure 13. Section of the polymeric chain of **7**.

state. In the asymmetric unit there are two chemically unique Cs cations, and TEMPO anions (Figure 11). The O(1)−Cs(2)−N(1) and the O(2)−Cs(2)−N(2) angles are 27.17(6)° and 27.33(6)°, respectively. Because of the increasing ionic radius of the alkali metal, hence its further distance from the N−O vector, the respective O−M−N angle decreases as Group 1 is descended. The repeating unit of the polymeric framework consists of a tetranuclear transoidal ladder arrangement of alternating Cs and O_{TEMPO} atoms. The two outer rings in this ladder deviate markedly from planarity (sum of angles, 355.48°), while the central ring (as a consequence of symmetry) is perfectly planar. Within the ladder, the Cs−O bond lengths vary dramatically [range, 2.713(2)−3.436(2) Å]. From a supramolecular perspective, the tetrameric ladders further associate to form [via a double ration of *inter*-ladder Cs(1)···O(1) contacts] a two-dimensional polymer chain (Figure 13). Formally, Cs(1) is only coordinated to O atoms; while Cs(2) is bound to two μ_3- and one μ_2-O (*intra*-ladder) and receives additional stabilization from the N(2) atoms of the TEMPO ligand. The Cs atoms are further stabilized by a series of Cs···C agostic interactions [range of bond distances, 3.498(3)−3.837-(3) Å]. To the best of our knowledge, **7** represents the first crystallographically characterized Cs nitroxide complex. Focusing on the $TEMPO^-$ ligand, the O center adopts a μ_3-bonding mode in complexes **2**−**7**. For TEMPO, this has previously only been observed in the TEMPO adduct of trimeric perfluoro-*o*-phenylene mercury.[36] Table 1 contains the X-ray crystallographic data for **1**−**7**.

NMR Spectroscopic Studies. The solubility of the alkali metal TEMPO complexes in D_8-THF solution (generally poorly soluble in arene solvent) allowed the complexes to be studied by NMR spectroscopy. Unfortunately, because of the fortuitous nature of the synthesis of **3** and lack of reproducibility of its synthesis, no solution characterization of this complex could be obtained. As NMR spectra of the new alkali metal complexes could be obtained, this provided further evidence that the TEMPO fragment was anionic in nature and not a neutral, paramagnetic radical species. The ^1H and ^{13}C NMR spectra for **1**, **2**, and **4**−**7** were recorded, and a summary of the data can be found in Tables 2 and 3, respectively.

Interestingly, given that the solid-state structures of the alkali metal TEMPO are so varied, the NMR spectroscopic data for the complexes in D_8-THF are essentially identical. This would seem to indicate that in polar solvent a solvent-separated ion pair or a solvated, lower oligomeric form of the complexes exist; in essence, the data show that the local coordination environment of the $TEMPO^-$ ligand is insensitive to the charge-balancing cation. Another plausible explanation for the uniformity of these results is that protonation of the TEMPO anion to TEMPO(H) (via deprotonation of the solvent medium or hydrolysis) could be taking place. To eliminate this scenario, a ^1H NMR spectrum of a D_8-THF solution of **6** was obtained (giving the resonances shown in Table 2).

Table 1. X-ray Crystallographic Data for **1**−**7**

	1	**2**	**3**	**4**	**5**	**6**	**7**
formula	$C_{44}H_{88}Li_4N_4O_6$	$C_{52}H_{104}N_4Na_4O_8$	$C_{52}H_{106}N_4Na_6O_{10}$	$C_{48}H_{104}N_8Na_4O_4$	$C_{52}H_{104}K_4N_4O_8$	$C_{48}H_{104}N_8O_4Rb_4$	$C_{36}H_{72}Cs_4N_4O_4$
M_r [g mol^{-1}]	796.94	1005.35	1085.35	949.35	1069.79	1199.27	1156.62
crystal system	monoclinic	monoclinic	triclinic	triclinic	triclinic	monoclinic	monoclinic
space group	$P2_1/n$	$P2_1/n$	$P\bar{1}$	$P\bar{1}$	$P\bar{1}$	$P2_1/c$	$C2/c$
a [Å]	11.3166(3)	15.7591(2)	11.6388(6)	11.5872(4)	10.9869(3)	11.6520(2)	24.5577(17)
b [Å]	10.9341(4)	17.0417(3)	11.8185(7)	12.6456(4)	15.4735(5)	23.8720(4)	8.9918(5)
c [Å]	19.4350(8)	21.7358(4)	13.1802(10)	20.7262(4)	18.5468(6)	22.2274(4)	22.9890(16)
α [deg]	90	90	75.977(3)	90.066(2)	78.9780(10)	90	90
β [deg]	94.438(2)	103.064(1)	85.990(2)	90.989(3)	84.851(2)	101.898(2)	116.892(1)
γ [deg]	90	90	69.221(3)	112.001(3)	74.592(2)	90	90
V [Å^3]	2397.61(15)	5686.32(16)	1644.28(18)	2815.28(14)	2981.14(16)	6049.87(18)	4527.4(5)
Z	2	4	1	2	2	4	4
ρ_{calcd} [g cm^{-3}]	1.104	1.174	1.096	1.120	1.192	1.317	1.697
$\mu(Mo_{K\alpha})$ [mm^{-1}]	0.070	0.103	0.107	0.097	0.349	3.260	3.233
measured refl.	24329	15937	8750	52741	24754	42115	8775
independent refl.	4901	8126	4554	13859	13358	10508	5112
R_{int}	0.043	0.0731	0.032	0.0381	0.0557	0.0388	0.0296
observed refl.	3371	6106	3329	9567	9092	6762	4354
parameters	270	629	335	662	645	601	225
$R1$ ($R1$ obs. data)	0.0480	0.1027	0.0495	0.0479	0.0560	0.0248	0.0275
$wR2$ ($wR2$ all data)	0.1168	0.2173	0.1199	0.1171	0.1418	0.0404	0.0670
max, min peaks [e Å^3]	0.347, −0.207	0.326, −0.299	0.229, −0.192	0.278, −0.252	0.710, −0.411	0.336, −0.329	1.140, −0.829

Table 2. ^{1}H NMR Spectroscopic Data[a] for **1**−**7**

	β-CH_2 and γ-CH_2 (TEMPO)	CH_3 (TEMPO)	CH_3 (TMEDA)	CH_2 (TMEDA)
TEMPO(D)	1.42, 1.33	1.19		
TMEDA			2.15	2.30
1	1.46	1.11		
2	1.45	1.10		
3				
4	1.44	1.06	2.15	2.30
5	1.42	1.00		
6	1.42	1.00	2.15	2.30
7	1.43	0.99		

[a] 400 MHz, 300 K, D_8-THF.

Table 3. ^{13}C NMR Spectroscopic Data[a] for **1**−**7**

	α-*C* (TEMPO)	β-*C*H$_2$ (TEMPO)	γ-*C*H$_2$ (TEMPO)	*C*H$_3$ (TEMPO)
1	58.9	41.2	18.6	19.2/34.3
2	58.5	41.4	18.8	18.8/34.6
3				
4	58.9	41.2	18.7	not obs.
5	58.4	41.7	18.7	18.7/35.6 (br)
6	58.9	41.4	18.9	18.5/34.5 (br)
7	58.3	41.2	18.9	19.2/34.5 (br)

[a] 100 MHz, 300 K, D_8-THF.

D_2O was then added to this solution to deuterate the TEMPO anion.[76] The subsequent ^{1}H NMR spectrum of this solution indicated that the shifts corresponding to the "new" TEMPO fragment differed significantly from those for **6** (Table 1). Akin to the data presented here, it has recently been shown that the NMR shifts for TMEDA-solvates of the sodium and potassium 2,2,6,6-tetramethylpiperidide (TMP) salts were essentially identical.[77] As the solution structures of each complex appear to be similar, they will be grouped together in this discussion.

The ^{1}H NMR spectra are relatively simple containing two broad resonances for the TEMPO anion at 0.99−1.11 (Me protons) and 1.42−1.46 ppm (overlap of β and γ protons). In general, the most upfield chemical shifts in these ranges were found for the TEMPO complexes containing the most electropositive alkali metals. The overlap of the β and γ-*H* atoms is consistent throughout the series, but in TEMPO(D) separate resonances are observed. As expected, for **4** and **6**, the ^{1}H NMR spectra reveal that on dissolution in D_8-THF, the TMEDA ligand is no longer coordinated to the respective metal center.

Turning to the ^{13}C NMR spectra provides an insight into the solution dynamics of the complexes (Table 3). In general, three sharp resonances [at 18.6−18.9 (γ-C), 41.2−41.7 (β-C), and 58.3−58.9 ppm (α-C)] are observed, along with two extremely broad signals at 18.5−19.2 and 34.3−35.6 ppm (the broad signals could not be observed for **4**). Using HSQC NMR spectroscopy, the broader signals can be attributed to two chemically distinct Me_{TEMPO} groups (Me groups are diastereotopic). This observation suggests that in D_8-THF solution, rotation about the O−N axis of the TEMPO$^-$ anion appears to be highly restricted, (hence two independent resonances) and rotation is slow on the NMR time scale. Unfortunately, because of the relatively low boiling point of D_8-THF, a high temperature NMR study could not be conducted.

(76) D_2O rather than H_2O was used to prevent swamping of the spectrum.
(77) Armstrong, D. R.; Graham, D. V.; Kennedy, A. R.; Mulvey, R. E.; O'Hara, C. T. *Chem.—Eur. J.* **2008**, *14*, 8025–8034.

Conclusions

Seven new alkali metal salts of $TEMPO^-$ have been prepared and characterized by X-ray crystallography and NMR spectroscopic studies. These reactions represent the first examples of elemental-metal reduction of the TEMPO radical to its anionic form. In the solid-state, the complexes adopt a wide variety of different structural motifs.

Acknowledgment. The authors thank the EPSRC (grant award no. EP/F065833/1) for generously sponsoring this research. This research was also supported by a Marie Curie Intra European Fellowship within the seventh European Community Framework Programme (PGA).

Supporting Information Available: X-ray crystallographic files in CIF format for **1**−**7**. This material is available free of charge via the Internet at http://pubs.acs.org.